Chemistry & Biology, Vol. 12, 217–228, February, 2005, ©2005 Elsevier Ltd All rights reserved. DOI 10.1016/j.chembiol.2004.12.006

Stereospecific Effects Determine the Structure of a Four-Way DNA Junction

Jia Liu,[1] Anne-Cécile Déclais,[1] Sean A. McKinney,[2] Taekjip Ha,[2] David G. Norman,[1] and David M.J. Lilley[1,*]

[1]Cancer Research UK Nucleic Acid Structure Research Group
MSI/WTB Complex
The University of Dundee
Dundee DD1 5EH
United Kingdom

[2]Physics Department
University of Illinois at Urbana-Champaign
1110 West Green Street
Urbana, Illinois 61801

Summary

Conversion of a centrally located phosphate group to an electrically neutral methyl phosphonate in a four-way DNA junction can exert a major influence on its conformation. However, the effect is strongly dependent on stereochemistry. Substitution of the *proR* oxygen atom by methyl leads to conformational transition to the stacking conformer that places this phosphate at the point of strand exchange. By contrast, corresponding modification of the *proS* oxygen destabilizes this conformation of the junction. Single-molecule analysis shows that both molecules are in a dynamic equilibrium between alternative stacking conformers, but the configuration of the methyl phosphonate determines the bias of the conformational equilibrium. It is likely that the stereochemical environment of the methyl group affects the interaction with metal ions in the center of the junction.

Introduction

Helical junctions [1] are important architectural elements in RNA, and the four-way DNA junction is the central intermediate in homologous genetic recombination [2]. The perfect (4H) junction is created by four double helices that are held together by the mutual exchange of strands (Figure 1A).

The junction adopts an extended geometry with four-fold symmetry (pseudo C_4) in the absence of added metal ions [3, 4]. It is induced to fold into the stacked X structure on addition of divalent metal ions such as Mg^{2+} (Figure 1A) [3, 5]. The structure was first proposed on the basis of electrophoretic [3, 6, 7], chemical probing [8], hydrodynamic [9], and FRET studies [5, 10], together with molecular modeling [11]. The stacked X structure is formed by the pairwise, coaxial stacking of helices to adopt a right-handed, antiparallel cross. Essentially all the conformational principles of this structure have been confirmed by recent crystallographic studies [12–18].

Formation of the stacked X structure from the open-square structure involves a lowering of symmetry from four- to two-fold. There are therefore two distinct conformers of the structure that are equivalent aside from the nucleotide sequence. This is illustrated for the junction shown schematically in Figure 1A. The four arms are sequentially labeled B, H, R, and X. These can undergo coaxial stacking in two alternative ways, either based on H stacking on B (and therefore R on X) in the *isoI* structure or B stacking on X (*isoII*). The component strands of the stacked X structure divide into two classes that interconvert on switching from the *isoI* to the *isoII* structure. The continuous strands (b and r in the *isoI* structure, drawn black) run the full length of the coaxially paired helices, while the exchanging strands (h and x in *isoI*) cross between the stacks, forming an exchange region at the center of the junction. In the *isoII* structure, the b and r strands become the exchanging strands, while h and x are now continuous. A single junction can sample both stacking conformers, with continual conformational exchange between structures. First suggested by experiments in bulk solution [19, 20], this has recently been demonstrated directly by single-molecule FRET spectroscopy [21, 22].

Electrostatic forces are extremely important in the folding of the four-way DNA junction, as indicated by the critical role for metal ions in the folding process. The formation of the stacked X structure requires either divalent metal ions [3, 5] or very high concentrations of monovalent ions [10, 23], and the rate of conformer exchange is strongly dependent on salt concentration [21, 22]. We have recently studied the role of phosphate charge using substitution by electrically neutral methyl phosphonates [24]. We found that if the central phosphate groups of the exchanging strands were rendered neutral by substitution, the resulting junction was substantially folded into the stacked X structure without addition of metal ions. We further found that the replacement of a single phosphate group lowered the requirement for metal ions in folding, and that the phosphate groups immediately 3′ and 5′ to the point of strand exchange also exerted a significant influence on the folding process. These experiments were carried out using the well-studied junction 3 [3], which is strongly biased to adopt the *isoII* conformation in which the b and r strands are exchanging. When the central phosphate groups of the h and x strands were replaced by methyl phosphonates, a fraction of the junction population adopted the *isoI* conformation [24]. The conformational switch that converts *isoII* to *isoI* results in the central phosphates of the h and x strands undergoing a marked change of environment, as they move from the duplex-like conformation of the continuous strands (P-P distance = 34 Å) to the point of strand exchange (P-P distance = 6.2 Å) (Figure 1A). The transition should lower the electrostatic repulsion between exchange-point phosphates, since the charge becomes removed from one or both. However, we noted that these junctions formed two distinct populations that did not interconvert. One fraction remained biased toward the *isoII* conformation (like the unmodified junction), while

*Correspondence: d.m.j.lilley@dundee.ac.uk

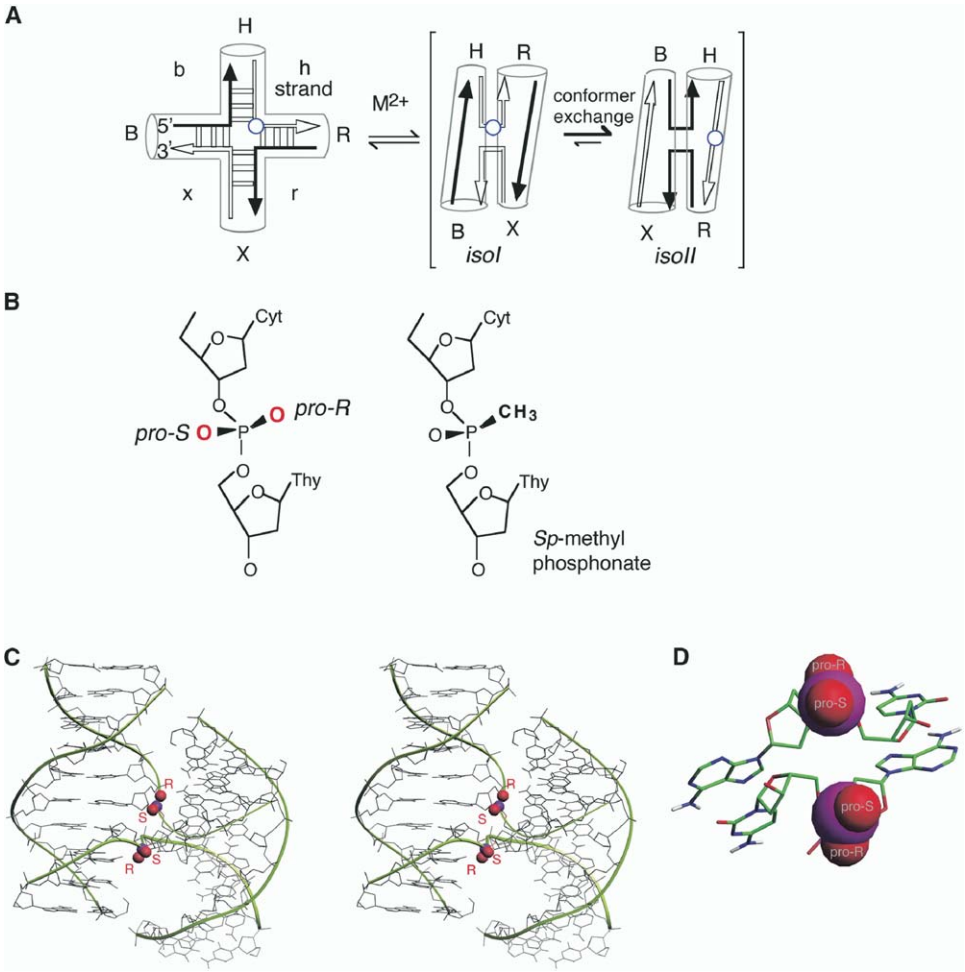

Figure 1. The Conformations of the Four-Way DNA Junction and the Chirality of the Phosphodiester Linkage

(A) The component strands of the junction are named b, h, r, and x; b and r are highlighted in black. The central phosphate group of the h strand is indicated by the open circle. On addition of metal ions, the junction folds into the stacked X structure, either in the *isoI* or *isoII* conformer. The highlighted phosphate is located at the point of strand exchange in *isoI* but on a continuous strand in *isoII*.

(B) The chiral properties of the phosphodiester linkage. The nonbridging oxygen atoms of the phosphodiester are prochiral, designated *proR* and *proS* as indicated. On substitution of an oxygen by methyl, the phosphorus becomes a chiral center. Note that replacement of the *proR* oxygen atom leads to an *Sp* configuration as illustrated.

(C) Parallel-eye stereoscopic view of the four-way junction, with the central phosphate groups at the point of strand exchange highlighted. The *proR* and *proS* oxygen atoms are indicated.

(D) Close-up space-filling view of the phosphate groups at the point of strand exchange. Note that the *proR* oxygen atoms are directed away from the center, while the *proS* oxygen atoms are relatively close together.

the other was now biased to the *isoI* conformation. We also noticed that a number of the junctions with methyl phosphonate substitutions at various positions migrated as two distinct species in polyacrylamide gels.

The absence of interconversion between the different species suggests a covalent difference between the modified junctions. The structures of phosphate and methyl phosphonate linkages are shown in Figure 1B. The two nonbridging oxygen atoms in a regular phosphodiester linkage are prochiral. Upon replacement of either the *proR* or *proS* oxygen, the phosphorus becomes a stereogenic center, and thus there are two inequivalent diastereomers of the methyl phosphonate. Confusingly, application of the Cahn-Ingold-Prelog rules for the assignment of configuration has the consequence that substitution of the *proR* oxygen atom leads to an *Sp* methyl phosphonate configuration, while substitution of the *proS* oxygen results in an *Rp* configuration. Oxidation of the methyl phosphonamidate during chemical synthesis can occur from either side, resulting in the formation of an approximately racemic mixture of *Rp* and *Sp* diastereomers. Since inversion of chirality at the phosphorus does not occur in the absence of a chemical reaction, our junctions will therefore contain the two distinct forms in equal quantities.

In the present work, we have investigated the conformational effect of a single, central methyl phosphonate substitution on the h strand of junction 3. We find that two distinct conformational species are present, and that these contain phosphorus centers with pure chiral-

ity. The conformational effects of the substitution are more subtle than the simple charge neutralization, and thus the prochirality of the nonbridging oxygen atoms is important in the conformation of the junction. This effect is likely to result from interactions with metal ions.

Results

Ion-Induced Folding of a Junction with a Single Methyl Phosphonate Group Centrally Located on a Continuous Strand

We have extensively studied the folding of a four-way junction termed junction 3 [3]. In the absence of any modification, this predominantly adopts the *isoII* conformation in a rapid exchange with approximately 20% of the molecules in the *isoI* conformation [21, 22]. In a recent study, we investigated the conformational effect of selective replacement of phosphate groups with methyl phosphonates [24]. Analysis of a junction in which the central phosphate groups of the continuous strands (i.e., strands h and x in the *isoII* conformation) were substituted by methyl phosphonate led us to conclude that there were two conformations present that did not interconvert, and we suspected that the origin of this effect lay in the stereochemistry of the modified phosphate groups. We have therefore analyzed a form of junction 3 in which just one of these phosphates has been substituted, that of the h strand. This phosphate becomes located at the point of strand exchange if the junction adopts the *isoI* conformation.

The component strands were made by chemical synthesis, and the junction was analyzed using the well-established method of comparative gel electrophoresis. In this approach, we generate the six possible forms of a given junction, having two long arms of 40 bp and two short arms of 14 bp, by hybridization of synthetic DNA species. We compare the electrophoretic mobility of the six species in polyacrylamide gels in buffer containing different concentrations of metal ions, from which the global shape of the junction can be deduced.

In Figure 2A, we compare the electrophoretic mobility pattern for the six long-short arm species of unmodified junction 3 (left) and that methyl phosphonate substituted at the center of the h strand (right). The electrophoresis was performed in buffer containing 5 μM (top) and 200 μM (bottom) Mg^{2+}. The unmodified junction gives the slow, intermediate, fast, fast, intermediate, slow pattern expected for a junction that predominantly adopts the *isoII* structure, as indicated on the left. At the lower Mg^{2+} concentration, the pattern indicates that the junction is about 80% folded (i.e., 20% is in the open square conformation), while it is fully folded at the higher ionic concentration.

The modified junction results in a very different pattern of mobilities, with the long-short arm species migrating as two species of similar intensity on the phosphorimage. An interpretation of the pattern observed in 5 μM Mg^{2+} is shown on the right, based on the presence of discrete fractions of junction in the *isoII* and *isoI* conformations, i.e., the pattern is a composite of slow, intermediate, fast, fast, intermediate, slow (*isoII*) and fast, intermediate, slow, slow, intermediate, fast (*isoI*). The modified phosphate group will be located on different kinds of strand in the two forms, i.e., on a continuous strand in *isoII* and an exchanging strand in *isoI*.

A Diametrically Opposite Methyl Phosphonate Substitution Has the Same Effect

If the nucleotide sequence of the junction is ignored, the stacked X structure has two-fold symmetry, and thus corresponding positions on the h and x strands are equivalent. If a subfraction of the h-strand-modified junction switches into the *isoI* conformation because it is energetically advantageous to place the neutral methyl phosphonate at the point of strand exchange, the same would probably be true for junction 3 substituted on the x strand. We therefore examined the electrophoretic mobility of the BH and HR species (as representative long-short arm species) in which the central phosphate of the x strand was replaced by methyl phosphonate (Figure 2B). These species are found to migrate as well-separated doublets, indicating that the same conformational effect resulted from this substitution. This is clearly the same process, and we have therefore concentrated exclusively on the h-strand-modified junction for the remainder of this study.

The Conformationally Different Forms of the Junction Contain Methyl Phosphonates of Opposite Chirality

When long-short arm junction species of different mobility are extracted from the polyacrylamide gel, they retain their characteristic mobility upon a second round of electrophoresis (data not shown). Thus, there is no interconversion between these species, indicating that the origin of the conformational difference is likely to be covalent. The most probable source of this difference seemed to lie in the chirality of the methyl phosphonate group, i.e., that the junctions biased toward the different stacking conformers are likely to contain opposite diastereomers. We therefore performed the following analysis, using the BX species of junction 3 containing a methyl phosphonate at the center of the h strand (Figure 3A). (1) The junction was separated into the fast- and slow-migrating species by polyacrylamide gel electrophoresis in the presence of 200 μM Mg^{2+}. The well-separated bands were excised, and the DNA was recovered by electroelution. (2) The DNA was digested to completion with phosphodiesterase I plus alkaline phosphatase. Every phosphodiester linkage in the DNA becomes hydrolyzed except for the methyl phosphonate, generating mononucleotides plus the methyl phosphonate-linked dinucleoside (dCmpT). We also synthesized the dCmpT dinucleoside methyl phosphonate de novo from cytosine methyl phosphonamidite to act as a standard. (3) The digest was analyzed by reversed-phase HPLC in order to resolve the two diastereomers of the methyl phosphonate-linked dinucleoside.

The degradation analysis was initially performed on isolated h strand containing the racemic methyl phosphonate linkage. The HPLC trace showed complete conversion into mononucleotides, plus smaller peaks corresponding to the two diastereomers of dCmpT (Supplemental Figure S1). The dinucleotide region is

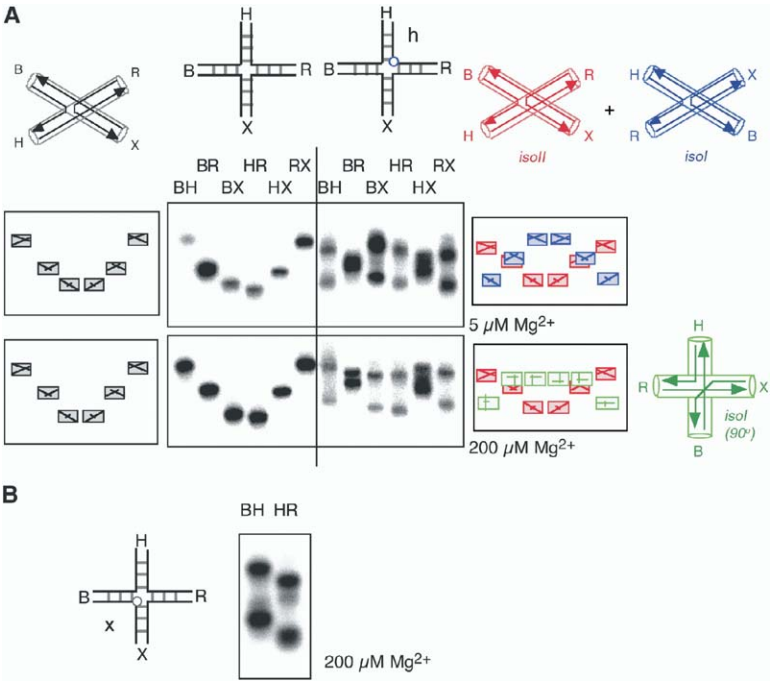

Figure 2. Analysis of the Conformation of a Four-Way DNA Junction by Comparative Gel Electrophoresis

In this method, we compare the electrophoretic mobility of the six species with two long and two short arms. These are named according to the long arms, e.g., species BH has long B and H arms, short R and X arms. (A) Analysis of junction 3 with a central methyl phosphonate substitution on the h strand. Electrophoresis was performed in 5 (upper) or 200 μM (lower) Mg^{2+}. The unmodified junctions (left) migrate as single species and give the usual slow, intermediate, fast, fast, intermediate, slow pattern of the *isoII* stacked X structure as illustrated on the left. By contrast, the methyl-phosphonate-containing junctions (right) each migrate as two species. This can be simply interpreted (shown on right) as a superposition of the patterns due to the junction in the stacked X-structure conformation in either the *isoI* (blue) or *isoII* (red) structure. In 200 μM Mg^{2+}, the *isoI* structure is best represented by a structure with a mean interaxial angle of 90° (green). (B) Analysis of the BH and HR species of junction 3 with a centrally located methyl phosphonate group on the x strand.

shown in Figure 3B (top trace). The two peaks eluting between 30 and 40 min were assigned as dCmpT for two reasons. First, they ran identically with the synthetic dCmpT; this was confirmed in experiments in which the digest and synthetic dinucleotide were mixed and reinjected, whereupon just two peaks were observed (data not shown). Second, following the HPLC separation, the putative dinucleotide species in the digest were subjected to electrospray mass spectrometry. The material from the two peaks gave masses of 530.22 and 530.21 compared to that calculated for the dimer of 530.16. We therefore conclude that the two peaks correspond to dCmpT in its two diastereomeric forms.

Next, the same analysis was performed on the two species of junction 3 BX that had been separated by electrophoresis in polyacrylamide, i.e., the slow (predominantly *isoI*) and fast (predominantly *isoII*) species. The dinucleotide region of the HPLC traces are shown in Figure 3B. We find that complete degradation of the separated junctions results in dinucleoside methyl phosphonates that migrate as single species. The faster-migrating junction species gives the dimer that elutes first, while the dinucleotide from the slower junction has the longer retention time. This indicates that the two forms of the junction electrophoretically separated by their conformational differences contain virtually pure diastereomers of the methyl phosphonate linkage, of opposite chirality. The separation of the junctions by electrophoresis had achieved a highly effective stereochemical resolution of the h strands. We conclude that the position of the methyl group on the phosphorus, replacing either the *proR* or *proS* oxygen atom, has a major conformational influence in determining the relative stability of the *isoI* and *isoII* stacking conformers. One diastereomer results in a dominant conformation that places the methyl phosphonate on a continuous strand (*isoII*), while the other stabilizes the alternative conformation where it is located at the point of strand exchange (*isoI*).

In passing, we note that the electrophoretic separation of four-way junctions with arms of unequal length provides a new way of resolving the diastereomers of potentially very long DNA molecules containing single methyl phosphonate linkages.

Determination of Absolute Stereochemistry of the Methyl Phosphonate Linkage

In order to relate our observations to the atomic structure of the four-way DNA junction, it was important to determine the absolute configuration of the methyl phosphonate group, i.e., to ascertain which nonbridging oxygen leads to the formation of the *isoI* stacking conformer when replaced by a methyl group. The configurations of a number of other methyl-phosphonate-linked dinucleosides have been determined by NMR [25–27] or crystallography [28–30] and correlated with HPLC retention times. In each case, the faster-eluting diastereomer has been the *Rp* form. The stereochemistry of the dCmpT dinucleotide has not previously been analyzed, and because of the critical importance of this to any structural conclusions from this work, we decided not to try to extrapolate from earlier assignments of other species. We therefore adopted the following strategy (Figure 4A). (1) The 8 nt oligonucleotide dGTACmpTGTC was synthesized containing a methyl phosphonate linkage at the unique CT step. This was separated into pure diastereomers by reversed-phase HPLC. Baseline separation of these species was achieved (Supplemental Figure S2). (2) The optically pure oligonucleotides were each hybridized to their complementary strand dGACAGTAC and studied by ^1H

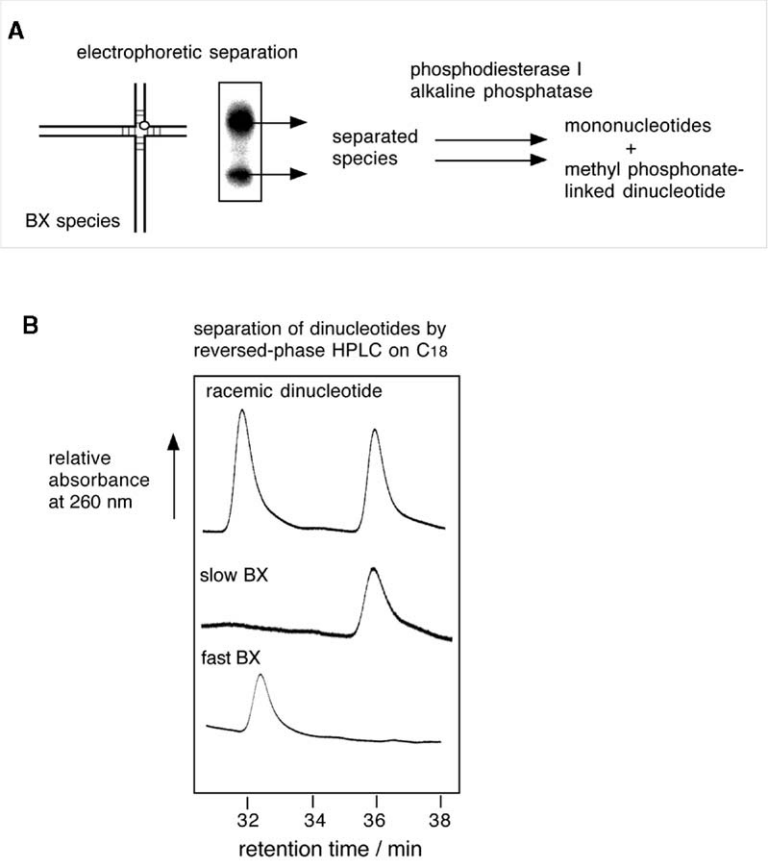

Figure 3. Junctions with Distinct Electrophoretic Mobilities Contain Methyl Phosphonates of Opposite Chirality

(A) The long-short arm junction 3 species BX with methyl phosphonate centrally located on the h strand were separated by gel electrophoresis in 200 μM Mg^{2+}. The fast- and slow-migrating DNA was purified by excision and electroelution and digested to completion with phosphodiesterase I and alkaline phosphatase. This leads to the breakage of all the phosphodiester linkages except for the methyl phosphonates, and the digest is separated by reversed-phase HPLC.

(B) The elution of the dCmpT dinucleotides from unseparated oligonucleotide (top) and BX species of slower and faster electrophoretic mobility (middle and bottom), respectively.

NMR. Using NOE measurements and a knowledge of the structure of double-stranded B-DNA, we were able to determine the absolute stereochemistry of the methyl phosphonate group in each duplex. Although the configuration of methyl phosphonates has been studied by NMR of single-stranded dinucleotides [27], we felt that placing the group in the context of B-form dsDNA was more reliable. (3) Each DNA sample was then subjected to phosphodiesterase digestion as above, and the mobility of the dCmpT dinucleotides was determined by reversed-phase HPLC.

Molecular models of the two diastereomers of a dCmpT dinucleoside methyl phosphonate in standard B-form geometry were constructed (Figure 4B) from which distances between the methyl attached to the phosphorus and base and sugar protons in the dinucleotide were measured (Supplemental Table S1). NOEs were measured from NOESY spectra of the two duplex species at 100 and 200 ms mixing times (Figure 4C) and classed on a scale from absent to strong. All are consistent with the assignment of the duplex containing the fast-eluting 8 nt oligonucleotide as the *Rp* diastereomer and that with the slower oligonucleotide as the *Sp*. In the following discussion of the NMR data, slow and fast refer to the relative elution speeds of the methyl-phosphonate-containing 8 nt single strand. Similarities in chemical shift prevented some NOEs from being measured, but a number of diagnostic contacts could be established.

Thymine H6

The most discriminating NOE is that between the methyl and H6 of the thymine (assignment B). This distance is calculated to be 3.2 Å for the *Sp* diastereomer, but 4.6 Å for the *Rp* form. The NOE was much stronger in the duplex formed from the slower oligonucleotide, i.e., slow >> fast.

Cytosine H1′

These distances (C) are predicted to be 5.1 and 4.1 Å for the *Rp* and *Sp* diastereomers, respectively. Both NOEs were relatively weak but were ordered slow > fast.

Thymine H4′, H5′, and H5″

The shortest predicted contact is that to H5″ (F) in the *Rp* diastereomer at 3.0 Å. This gives a strong NOE in the fast species, with fast > slow. The next shortest is to H5′ (G) at 4.2 Å in the *Rp* diastereomer. This gives a medium-strength NOE in the fast species but weak in the slow species. A significant contact with the H4′ (E) proton is only expected in the *Rp* diastereomer; an NOE was only observed in the fast species.

Cytosine and Thymine H3′

In principle, these interactions would discriminate very well between the diastereomers, but unfortunately the chemical shifts of the 3′ protons of the two nucleotides are identical, preventing unambiguous assignment (D). Nevertheless, the observed NOEs are consistent with the fast = *Rp* conclusion. The shortest distance is the cytosine H3′ in the *Sp* form at 3 Å, and the strongest

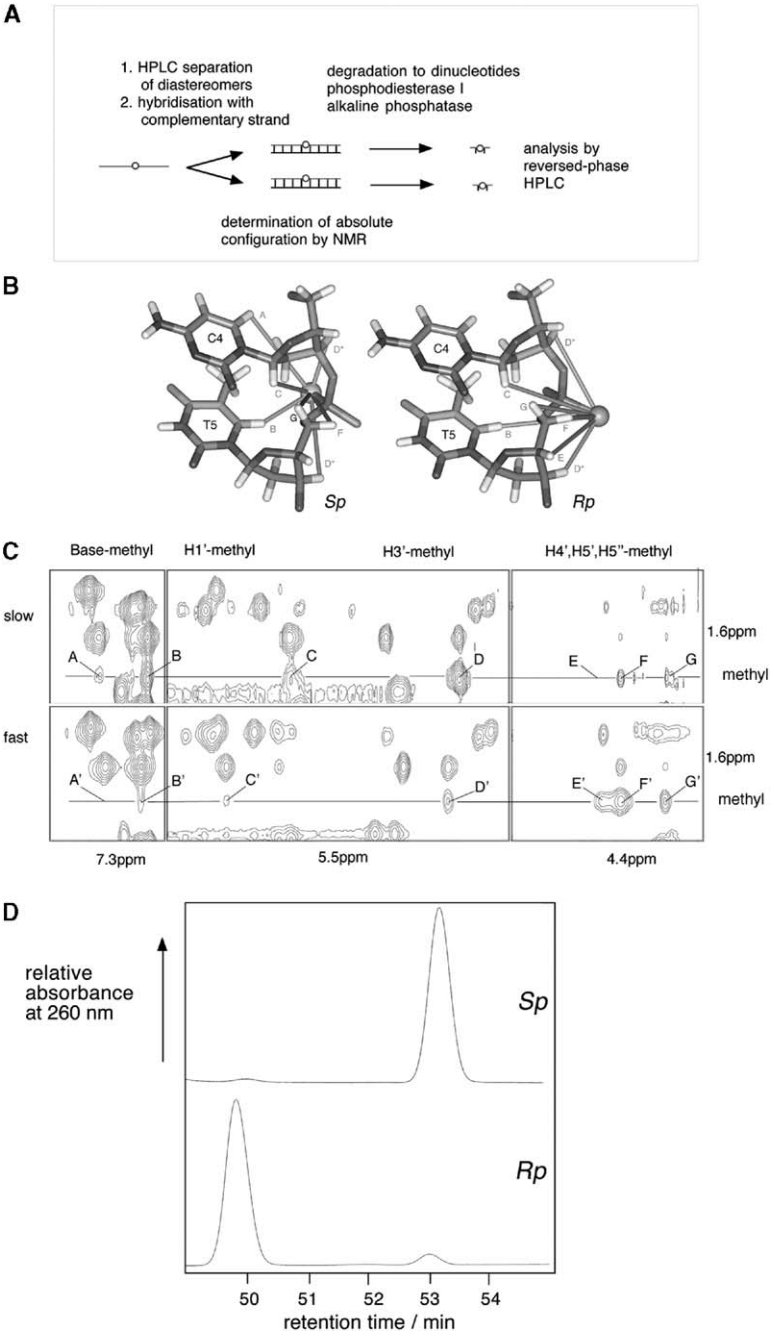

Figure 4. The Absolute Configuration of a Methyl-Phosphonate-Linked Dinucleoside by NMR Spectroscopy

(A) The diastereomers of the oligonucleotide GTACmpTGTC were separated by reversed-phase HPLC. These were each hybridized with their complement, and the resulting duplexes were studied by NMR in order to deduce the absolute configuration of their methyl phosphonate groups. They were then digested to completion with phosphodiesterase I and alkaline phosphatase, and the dCmpT dinucleotides were analyzed by HPLC.

(B) Proton-proton distances from the methyl phosphonate of dCmpT in *Rp* and *Sp* configurations in B-form conformation.

(C) NOESY spectra of the methyl base, H1′, H3′, and H4′, H5′, H5″ contacts for the duplex species constructed from the oligonucleotides with slow (upper) and fast (lower) HPLC elution times.

(D) HPLC profiles of the digested DNA correlated with the methyl phosphonate configurations assigned by NMR.

NOE is found in the slow species. The next shortest distance is the thymine H3′ in the *Rp* form at 3.3 Å, and a medium-strength NOE is observed in the fast species.

All the available NMR data support the conclusion that the faster 8 nt DNA contained the *Rp* linkage. Some differences in chemical shift and NOE intensity were found in positions close to the methyl phosphonate, consistent with a degree of structural perturbation arising from the substitution. These are likely to be relatively minor, however, and we feel that the use of the B-DNA framework for the interpretation of the data is reliable. In fact, the use of seven points of agreement in the analysis of the NOE data makes the final assignment of stereochemistry extremely robust.

After completion of the NMR studies, each 8 bp duplex was digested to completion with phosphodiesterase I and alkaline phosphatase, and the digests were separated by reversed-phase HPLC as before (Figure 4D). The duplex containing the *Rp* methyl phosphonate gave rise to a dCmpT dimer with a shorter retention time (i.e., eluted faster) than that from the duplex with the *Sp* methyl phosphonate (summarized in Table 1). This now allows us to assign the chirality of the methyl phosphonate linkages in our four-way junctions.

Table 1. Summary of the Electrophoretic and HPLC Migration Properties of Different Species as a Function of Methyl Phosphonate Stereochemistry

8-mer[a] HPLC	Configuration NMR	Dimer[b] HPLC	BX Junction Electrophoresis	BR Junction Electrophoresis	Conformer Bias Single Molecule
fast	*Rp* (*proS* modified)	fast	fast (i.e., *isoII*)	fast	*isoII* >> *isoI*
slow	*Sp* (*proR* modified)	slow	slow (i.e., *isoI*)	slow	*isoI* > *isoII*

HPLC elution speeds, electrophoretic mobilities, and conformer bias observed by single-molecule FRET studies and the methyl phosphonate configuration determined by NMR. This allows all the studies in this work to be correlated.
[a] Relative elution speeds of dGTACmpTGTC on reversed-phase HPLC.
[b] Relative elution speeds of dCmpT on reversed-phase HPLC.

Single-Molecule FRET Spectroscopy Reveals Two Species with Distinct Conformational Dynamics

We have used single-molecule fluorescence resonance energy transfer (FRET) experiments to investigate further the different conformational populations present in the methyl-phosphonate-substituted junction. In these experiments, we study a version of junction 3 sequence having four arms of 22 bp, with the central phosphate of the h strand substituted by methyl phosphonate. Cy3 is attached to the 5′ terminus of the b strand, while Cy5 is attached to the 3′ terminus of the r strand, thus placing the fluorescent donor and acceptor at the ends of the B and X arms, respectively. The molecules are tethered to a glass coverslip via biotin that was attached to the 5′ terminus of the r strand and studied using confocal scanning microscopy [31]. In the *isoII* conformation, the fluorophores are spaced far apart (giving low FRET efficiency), while in the *isoI* conformation they are closer together (higher FRET efficiency). Using this approach, we have shown previously rapid interconversion between the *isoI* and *isoII* conformers in unmodified junction 3 [21], with a population that is biased to the *isoII* conformation as observed by ensemble experiments including comparative gel electrophoresis.

In initial experiments, the junctions contained a racemic methyl phosphonate linkage. The single-molecule analysis performed in the presence of 10 mM Mg^{2+} revealed two distinct classes of molecules, biased toward high and low FRET efficiency (data not shown), which were assumed to correspond to the two stereochemical forms. We therefore decided to purify these at the outset, using our gel electrophoretic separation of the BX species as a means of resolution. By this means, we separated the 22 bp h strand into the two diastereomeric forms; these were then hybridized with the appropriately Cy3-, Cy5-, and biotin-labeled strands (Figure 5A). Single-molecule time records for examples of single junctions show that both species exhibit rapid and frequent transitions between high and low FRET states, but with clearly distinct biases between the two states (Figures 5B and 5C). Histograms of the cumulative duration at different FRET efficiencies (Figures 5D and 5E) show that both forms of the junction spent time in one of two conformations, with FRET efficiencies distributed about means of 0.2 and 0.55. However, there was a significant difference in bias for the two forms. The junction containing the *Rp* methyl phosphonate linkage was strongly biased to the low FRET state, i.e., the *isoII* conformation. This is consistent with the faster electrophoretic migration of the BX species containing this linkage. By contrast, the high and low FRET states were more evenly populated in the junction containing the *Sp* linkage, with a bias toward the high FRET state, i.e., the *isoI* conformation. This agrees with the slower migration of the BX species containing this linkage. The behavior of individual junction molecules was quite homogeneous. A plot of the average duration in the high and low FRET states for individual molecules of racemic junctions (Figure 5F) shows a distribution of dwell times. However, this separates into two distinct, well-grouped sets when the methyl phosphonate linkages are resolved (Figure 5G); the majority of the *Rp* junctions having dwell times low > high FRET, while for most of the *Sp* junctions the dwell times are more even but biased high > low FRET. There are a few molecules that lie outside these groupings, probably resulting from imperfect electrophoretic separation of diastereomeric forms. It is important to note that, despite the different bias of the junctions with stereochemistry, both species populate both stacking conformers and frequently interconvert. The transition rates are within a factor of 2 or 3 from those of unmodified junctions, suggesting that free energy barriers against stacking conformer transitions are not grossly altered.

The Structure of the *isoI* Conformer of the Junction at Higher Mg^{2+} Concentrations

The analysis by comparative gel electrophoresis of the structure of junction 3 modified centrally on the h strand was interpreted in terms of a composite of the electrophoretic patterns of the *isoI* and *isoII* conformations, each adopting the stacked X structure (Figure 2A, top). However, as the Mg^{2+} concentration was raised to 200 μM or higher, the pattern changed in a more subtle way. Under these conditions, the BR and HX species each split into a better-defined doublet, and the slower species were similar in mobility to the slower BX and HR species. We analyzed the methyl phosphonate stereochemistry in the two BR species by enzymatic digestion and HPLC of the dCmpT species as before. The BR species with faster electrophoretic mobility was found to contain the *Rp* methyl phosphonate linkage (faster-eluting HPLC), while the species with slower electrophoretic mobility contained the *Sp* linkage (Supplemental Figure S4). We can therefore conclude that the junction species with fast mobility corresponds to the predominantly *isoII* conformation, while the slower species is biased to the *isoI* conformation. Thus, the electrophoretic pattern of the *isoII* species is typical of the antiparallel stacked X structure. By contrast, the

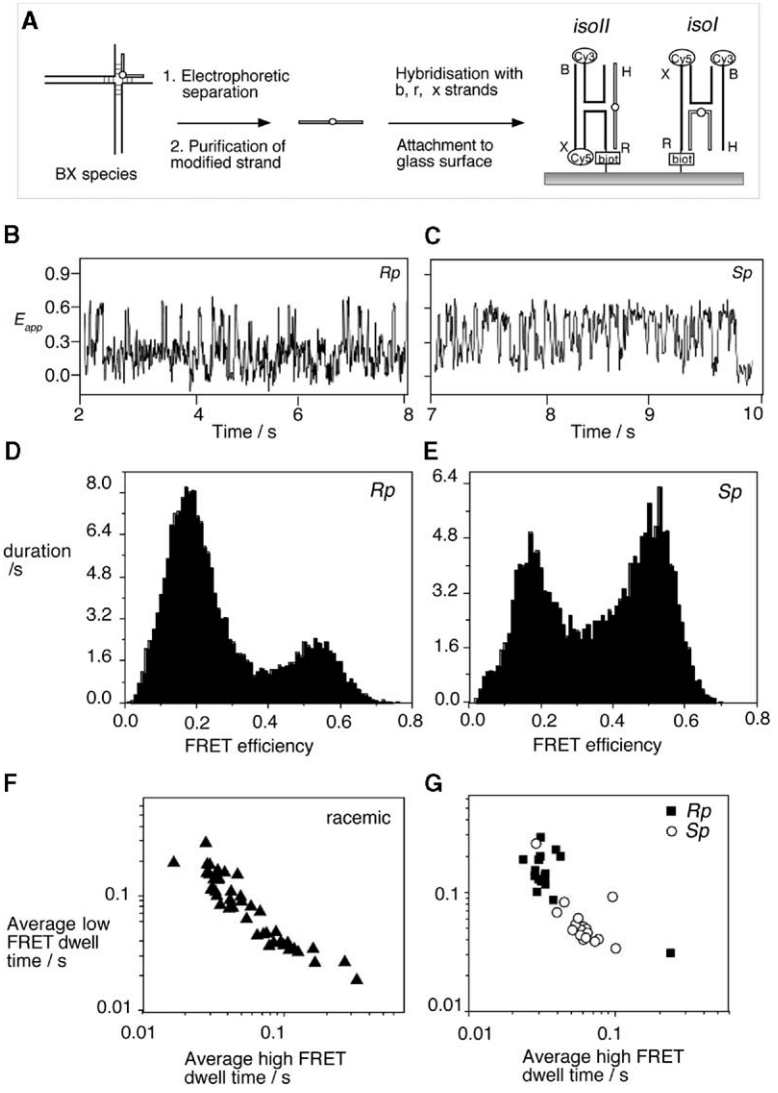

Figure 5. Single-Molecule Stacking Conformer Dynamics in Junctions Containing a Single Methyl Phosphonate

(A) The diastereomers of an h strand with a central methyl phosphonate group were separated by gel electrophoresis of a junction 3 BX species. The individual h strands were separately hybridized to new b, r, and x strands to generate junctions with 5′ biotin (R arm), 5′ Cy3 (B arm), and 3′ Cy5 (X arm) and attached to the surface of a glass coverslip. These were then studied by single-molecule FRET spectroscopy. Note that the Cy3 (donor) and Cy5 (acceptor) are physically close in the *isoI* conformation, giving efficient energy transfer, whereas they are far apart in *isoII*, thus lowering FRET efficiency.

(B and C) Representative records of FRET efficiency (E_{app}) in the presence of 10 mM Mg^{2+} as a function of time for single molecules of junction 3 with *Rp* (B) and *Sp* (C) methyl phosphonate groups. Note that both species undergo frequent transitions between the high and low FRET states.

(D and E) Histograms of E_{app} combining all data time points from 35 molecules for junctions containing methyl phosphonate in the *Rp* (D) and *Sp* (E) configuration. Both junctions have two populations with mean FRET efficiencies of 0.2 and 0.55, corresponding to the *isoII* and *isoI* conformations, respectively.

(F and G) Plots of average durations in the high and low FRET states for junction with unresolved (F) and for the those with resolved methyl phosphonate groups (G), where the data for the *Rp* diastereomers are shown by the filled squares (16 molecules), and those for the *Sp* (19 molecules) diastereomers are shown by the open circles. Each symbol represents averaging over one junction molecule. With the two outlying points removed, the mean dwell times calculated are 33 and 166 ms for the high and low FRET states of the *Rp* diastereomers, respectively, and 68 and 53 ms for the high and low FRET states of the *Sp* diastereomers, respectively.

isoI-biased species gives a fast, slow, slow, slow, slow, fast pattern consistent with a mean interaxial angle toward 90° (Figure 2A, bottom).

Discussion

Substitution of a single phosphate group by a methyl phosphonate can have a major influence on the conformation of a four-way junction, facilitating the ion-induced folding of the junction by pairwise coaxial stacking and changing the relative stability of alternative stacking conformers. However, this phenomenon clearly operates at a number of levels.

First, the substitution results in the loss of a negative charge from a critical phosphate group. In the example studied here, we have replaced the central phosphate group of the h strand, which is a continuous strand in the predominant *isoII* conformer of unmodified junction 3 [3, 10, 21]. Electrostatic interactions are extremely important in branched nucleic acids, and charge screening by cations is normally essential to permit folding to occur. In the absence of added metal ions, the unmodified four-way DNA junction cannot fold into the stacked X structure and remains in the extended open-square structure [3, 4]. Crystal structures of four-way junctions [12–18] show that there is a clustering of phosphate groups around the point of strand exchange, and it is likely that a reduction in the electrostatic repulsion between these negative charges will be essential for the stacked X structure to become stable. We have recently shown that, when both central phosphate groups of the exchanging strands are neutralized by methyl phosphonate substitution, the junction folds in the absence of added metal ions [24]. Once a junction becomes folded into the stacked X structure, there is a rapid, dynamic exchange between alternative stacking conformers [21, 22]. The position of the conformational equilibrium will be governed by the relative stability of the two conformers, which will depend on the local base sequence. Some junctions (such as junction 7 [20]) are very weakly biased with closely similar populations of both conformers, while junction 3 is biased to-

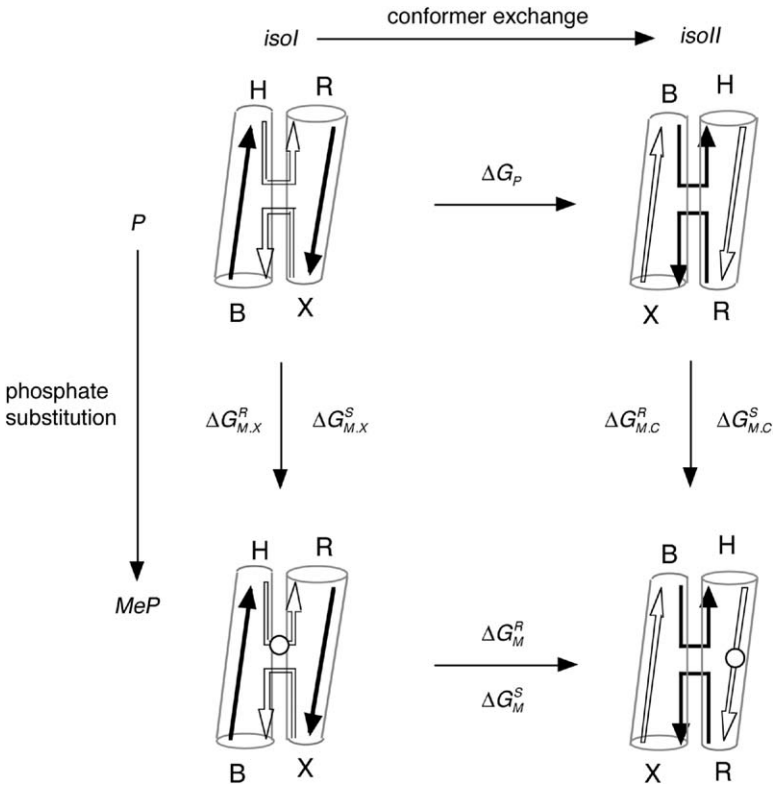

Figure 6. Thermodynamic Cycles for Conformer Exchange in an Unmodified Four-Way Junction and One with a Single Central Methyl Phosphonate in either *Rp* or *Sp* Configuration

Horizontal transformations are conformer transitions, and vertical transformations are the conversion of phosphate to methyl phosphonate. The free energies for the individual steps are indicated, where the subscripts denote the following: P, phosphate; M, methyl phosphonate; X, exchanging strand; C, continuous strand. Superscripts R and S denote *Rp* and *Sp* configurations, respectively. The signs of the free energies are given for the directions *isoI* to *isoII* and phosphate to methyl phosphonate, as shown by the arrows.

ward the *isoII* conformer. In the absence of phosphate group modification, the position of the *isoI*-*isoII* equilibrium should not be influenced by electrostatics, because the interactions between phosphates should be closely similar for both conformers; we have observed previously that the position of equilibrium is unaffected by Mg^{2+} concentration [21]. However, when one of the central phosphate groups is neutralized by methyl phosphonate substitution, that no longer remains the case, and a significant electrostatic term is introduced into the free energy difference between the conformers. Thus, the central phosphate group of the h strand will be located at the point of strand exchange in the *isoI* conformer, while it will be more distantly located on a continuous strand in the *isoII* conformer. This could perturb the position of equilibrium toward the otherwise disfavored *isoI* conformer because the electrostatic potential is reduced by placing the neutralized phosphate group at the point of strand exchange.

However, the effects that we have observed are clearly more subtle than the simple removal of a negative charge from a critical phosphate group. Substitution of the alternative prochiral nonbridging oxygen atoms led to very different conformational effects on the junctions, despite having the same overall electrical charge. Figures 1C and 1D show the location of the central phosphate groups on the exchanging strands of the crystal structure of the four-way junction determined by Ho and coworkers [14]. The two central phosphate groups of the exchanging strands face each other across the minor groove side of the junction, with a P-P distance of 6.2 Å. However, the nonbridging oxygen atoms lie in very different environments. While the *proS* oxygen atoms project laterally from the minor groove side with an O-O distance of 5.9 Å, the *proR* oxygen atoms are directed away from the center of the junction with an O-O distance of 9.0 Å. This difference has profound conformational consequences for the conformation of the junction. Replacement of one of the *proR* oxygen atoms by a methyl group, with consequent neutralization of phosphate charge, results in a significant stabilization of the *isoI* conformation, whereas the conformer bias is heavily toward the *isoII* conformation upon substitution of a *proS* oxygen atom.

We can construct two thermodynamic cycles (Figure 6) based on the free energy for conformer exchange (*isoI* to *isoII*) for the unmodified junction (ΔG_P) and that modified by a central *Rp* or *Sp* methyl phosphonate (ΔG_M^R and ΔG_M^S, respectively). The remaining terms in the cycle are the conversion of an exchange point phosphate to *Rp* or *Sp* methyl phosphonate ($\Delta G_{M.X}^R$ and $\Delta G_{M.X}^S$, respectively) and the corresponding conversion of the central phosphate of the continuous strand ($\Delta G_{M.C}^R$ and $\Delta G_{M.C}^S$, respectively). Summing around the cycles shows that $\Delta G_P - \Delta G_M^R - \Delta G_{M.X}^R + \Delta G_{M.C}^R = 0 = \Delta G_P - \Delta G_M^S - \Delta G_{M.X}^S + \Delta G_{M.C}^S$ The terms of most interest are the change in free energy by conversion of an exchange point phosphate to an *Rp* or *Sp* methyl phosphonate, given by $\Delta G_{M.X}^R = \Delta G_P - \Delta G_M^R + \Delta G_{M.C}^R$ and $\Delta G_{M.X}^S = \Delta G_P - \Delta G_M^S + \Delta G_{M.C}^S$.

The conformational equilibrium for the unmodified junction is biased toward the *isoII* structure ($K_{conf} = 3.4$) with a free energy of $\Delta G_P = -2.9$ kJ mol^{-1} [21]. ΔG_M^R and ΔG_M^S can be determined from the conformational

equilibria observed as the ratio of dwell times in the present single-molecule studies. The energetics of converting a phosphate group on a continuous strand ($\Delta G_{M.C}^{R}$ and $\Delta G_{M.C}^{S}$) are not known. However, studies on the thermal melting of modified duplex species indicate that both diastereomers are destabilizing, with the larger effect coming from the *Sp* modification [25, 32], i.e., both free energies are positive, and $\Delta G_{M.C}^{S} > \Delta G_{M.C}^{R}$.

Substitution of the *proR* oxygen atom of the central phosphate (*Sp* methyl phosphonate) leads to a junction that is now biased to the *isoI* conformer, with K_{conf} = 0.8 corresponding to ΔG_{M}^{S} = 560 J mol^{-1}. Thus, the effect of converting the exchange point phosphate to an *Sp* methyl phosphonate is $\Delta G_{M.X}^{S} = -2.9 - 0.6 + \Delta G_{M.C}^{S} = -3.5 + \Delta G_{M.C}^{S}$.

Because $\Delta G_{M.C}^{S}$ is positive, we conclude that $-\Delta G_{M.X}^{S} < 3.5$ kJ mol^{-1}. Since the *proR* oxygen is directed away from the center of the junction, this is probably dominated by the energetics of simple charge neutralization.

Substitution of the *proS* oxygen atom of the central phosphate (*Rp* methyl phosphonate) is more complex. The single-molecule dwell times show that the modified junction is slightly more biased toward *isoII* than the unmodified junction, with K_{conf} = 5.0 corresponding to ΔG_{M}^{R} = −3.9 kJ mol^{-1}. Thus, the detrimental effect of replacing a *proS* oxygen atom with a methyl group more than offsets the lowering of free energy that should result from the reduction in electrostatic repulsion on removing the charge from an exchange-point phosphate group: $\Delta G_{M.X}^{R} = -2.9 + 3.9 + \Delta G_{M.C}^{R} = +1.0 + \Delta G_{M.C}^{R}$.

Since $\Delta G_{M.C}^{R}$ is positive, the effect of converting the exchange-point phosphate to an *Rp* methyl phosphonate is net destabilizing, i.e., $\Delta G_{M.X}^{R} > 1$ kJ mol^{-1}.

It is somewhat surprising that the substitution of the *proS* oxygen (i.e., an *Rp* methyl phosphonate) is so destabilizing at the point of strand exchange. A methyl-oxygen steric clash at the center of the junction is improbable given the similarity in size of an oxygen atom and a methyl group and the distance between the *proS* oxygen atoms. It therefore seems more likely that a methyl group at the *proS* position interferes with ionic interactions at the center of the junction. There is a significant cluster of phosphate groups in this region that includes a well-defined box of four phosphates on the minor-groove side of the junction, comprising the central phosphates and those immediately to their 3′ side [24]. There is a high probability of occupancy by a metal ion (probably as diffuse binding), which could be important for general charge screening in this region. If this is hindered by the replacement of one of the *proS* oxygen atoms by a methyl group, the loss of this positively charged ion could be more important than the removal of the negative charge from a single phosphate group.

In addition to the influence of phosphate modification on conformer bias, we have also seen that the geometry of the junction appears to be altered by the presence of the methyl phosphonate. The electrophoretic pattern of the *isoI*-biased structure containing the *Sp* methyl phosphonate can most readily be interpreted in terms of an interaxial angle of 90°, although this will be a mean value if the individual conformers have some flexibility. The apparent FRET efficiency of the high FRET species containing *Sp* and *Rp* methyl phosphonate groups were closely similar, indicating that the interfluorphore distance is not greatly changed. While we do not fully understand this at present, it is possible that the rotation of the axes is accompanied by other changes in local conformation that result in a preservation of the distance. We have previously found that introduction of a discontinuity in the backbone at the point of strand exchange leads to a very similar 90° interaxial angle judged by comparative gel electrophoresis [33]. However, this was not a result of the removal of the phosphate because the geometry was the same with or without a 5′ phosphate group at the nick.

Significance

It is likely that the kinds of electrostatic and stereochemical effects described here will be important in branched nucleic acids generally. Helical junctions are common architectural elements in RNA molecules [1] and play a particularly important role in the conformation of small, autonomously folding RNA species as exemplified by the hairpin ribozyme [34–37]. Metal ions are essential for the folding of these molecules, and bound ions can also serve a functional role such as catalysis. The kind of approaches used in these studies of DNA junctions could fruitfully be applied to the analysis of RNA folding.

Experimental Procedures

Full details of all experimental methods are given in the Supplemental Data.

Synthesis of Oligonucleotides

Oligodeoxyribonucleotides were synthesized using standard phosphoramidite chemistry and purified as described previously [24].

Construction of Junctions for Analysis by Comparative Gel Electrophoresis

The analysis was performed as described in [24], using junction 3; the sequence is given in the Supplemental Data.

Enzymatic Degradation of Oligonucleotides and Separation of Methyl-Phosphonate-Linked Dinucleosides

DNA was digested with 2 U/μmol DNA each of phosphodiesterase I and shrimp alkaline phosphatase. The digests were subjected to reversed-phase HPLC separation.

NMR Spectroscopy of DNA

dGTACmpTGTC and its complement dGACAGTAC were synthesized and purified by reversed-phase HPLC before removal of 5′-DMT groups. Methyl phosphonate diastereomers were resolved by a second round of reversed-phase HPLC using a gradient of 1%–15% acetonitrile in 0.1 M TEAA (Supplemental Data). One- and two-dimensional NMR spectra were acquired in D_2O at 500 MHz.

Single-Molecule Spectroscopy

Oligonucleotides for single-molecule spectroscopy were prepared separately, with fluorophores attached to nonmethyl-phosphonate-modified strands. Cy3 was coupled to the 5′ terminus of the b strand as a phosphoramidite. The r strand was prepared with biotin coupled to the 5′ terminus and Cy5 conjugated to the 3′ terminus via an aminolinker. Oligonucleotides were purified by electrophoresis, and fluorophore-labeled oligonucleotides were further purified by reversed-phase HPLC. The methyl-phosphonate-containing h

strand was recovered from the electrophoretic separation of the BX junction species as described in the main text. The sequences are given in the Supplemental Data. Single-molecule fluorescence data were acquired using a confocal scanning microscope [21, 22]. Apparent FRET efficiency (E_{app}) was calculated as the acceptor intensity divided by the sum of donor and acceptor intensities.

Supplemental Data

Supplemental Data, including two tables, four figures, and Supplemental Experimental Procedures are available at http://www.chembiol.com/cgi/content/full/12/2/217/DC1/.

Acknowledgments

We thank Timothy Wilson for discussion, Zheng-Yun Zhao for chemical synthesis of modified oligonucleotides, Linda Morris for mass spectrometry, and Cancer Research-UK (United Kingdom) and the National Science Foundation (United States) for financial support.

Received: September 18, 2004
Revised: November 8, 2004
Accepted: December 3, 2004
Published: February 25, 2005

References

1. Lilley, D.M.J. (2000). Structures of helical junctions in nucleic acids. Q. Rev. Biophys. *33*, 109–159.
2. Holliday, R. (1964). A mechanism for gene conversion in fungi. Genet. Res. *5*, 282–304.
3. Duckett, D.R., Murchie, A.I.H., Diekmann, S., von Kitzing, E., Kemper, B., and Lilley, D.M.J. (1988). The structure of the Holliday junction and its resolution. Cell *55*, 79–89.
4. Clegg, R.M., Murchie, A.I.H., Zechel, A., and Lilley, D.M.J. (1994). The solution structure of the four-way DNA junction at low salt concentration; a fluorescence resonance energy transfer analysis. Biophys. J. *66*, 99–109.
5. Murchie, A.I.H., Clegg, R.M., von Kitzing, E., Duckett, D.R., Diekmann, S., and Lilley, D.M.J. (1989). Fluorescence energy transfer shows that the four-way DNA junction is a right-handed cross of antiparallel molecules. Nature *341*, 763–766.
6. Gough, G.W., and Lilley, D.M.J. (1985). DNA bending induced by cruciform formation. Nature *313*, 154–156.
7. Cooper, J.P., and Hagerman, P.J. (1987). Gel electrophoretic analysis of the geometry of a DNA four-way junction. J. Mol. Biol. *198*, 711–719.
8. Kimball, A., Guo, Q., Lu, M., Cunningham, R.P., Kallenbach, N.R., Seeman, N.C., and Tullius, T.D. (1990). Construction and analysis of parallel and antiparallel Holliday junctions. J. Biol. Chem. *265*, 6544–6547.
9. Cooper, J.P., and Hagerman, P.J. (1989). Geometry of a branched DNA structure in solution. Proc. Natl. Acad. Sci. USA *86*, 7336–7340.
10. Clegg, R.M., Murchie, A.I.H., Zechel, A., Carlberg, C., Diekmann, S., and Lilley, D.M.J. (1992). Fluorescence resonance energy transfer analysis of the structure of the four-way DNA junction. Biochemistry *31*, 4846–4856.
11. von Kitzing, E., Lilley, D.M.J., and Diekmann, S. (1990). The stereochemistry of a four-way DNA junction: a theoretical study. Nucleic Acids Res. *18*, 2671–2683.
12. Nowakowski, J., Shim, P.J., Prasad, G.S., Stout, C.D., and Joyce, G.F. (1999). Crystal structure of an 82 nucleotide RNA-DNA complex formed by the 10–23 DNA enzyme. Nat. Struct. Biol. *6*, 151–156.
13. Ortiz-Lombardía, M., González, A., Erijta, R., Aymamí, J., Azorín, F., and Coll, M. (1999). Crystal structure of a DNA Holliday junction. Nat. Struct. Biol. *6*, 913–917.
14. Eichman, B.F., Vargason, J.M., Mooers, B.H.M., and Ho, P.S. (2000). The Holliday junction in an inverted repeat DNA sequence: Sequence effects on the structure of four-way junctions. Proc. Natl. Acad. Sci. USA *97*, 3971–3976.
15. Eichman, B.F., Mooers, B.H.M., Alberti, M., Hearst, J.E., and Ho, P.S. (2001). The crystal structures of psoralen cross-linked DNAs: drug-dependent formation of Holliday junctions. J. Mol. Biol. *308*, 15–26.
16. Vargason, J.M., and Ho, P.S. (2002). The effect of cytosine methylation on the structure and geometry of the Holliday junction: the structure of d(CCGGTACm5CGG) at 1.5 Å resolution. J. Biol. Chem. *277*, 21041–21049.
17. Hays, F.A., Vargason, J.M., and Ho, P.S. (2003). Effect of sequence on the conformation of DNA Holliday junctions. Biochemistry *42*, 9586–9597.
18. Thorpe, J.H., Gale, B.C., Teixeira, S.C., and Cardin, C.J. (2003). Conformational and hydration effects of site-selective sodium, calcium and strontium ion binding to the DNA Holliday junction structure $d(TCGGTACCGA)_4$. J. Mol. Biol. *327*, 97–109.
19. Miick, S.M., Fee, R.S., Millar, D.P., and Chazin, W.J. (1997). Crossover isomer bias is the primary sequence-dependent property of immobilized Holliday junctions. Proc. Natl. Acad. Sci. USA *94*, 9080–9084.
20. Grainger, R.J., Murchie, A.I.H., and Lilley, D.M.J. (1998). Exchange between stacking conformers in a four-way DNA junction. Biochemistry *37*, 23–32.
21. McKinney, S.A., Déclais, A.-C., Lilley, D.M.J., and Ha, T. (2003). Structural dynamics of individual Holliday junctions. Nat. Struct. Biol. *10*, 93–97.
22. Joo, C., McKinney, S.A., Lilley, D.M.J., and Ha, T. (2004). Exploring rare conformational species and ionic effects in DNA Holliday junctions using single-molecule spectroscopy. J. Mol. Biol. *341*, 739–751.
23. Duckett, D.R., Murchie, A.I.H., and Lilley, D.M.J. (1990). The role of metal ions in the conformation of the four-way junction. EMBO J. *9*, 583–590.
24. Liu, J., Déclais, A.-C., and Lilley, D.M.J. (2004). Electrostatic interactions and the folding of the four-way DNA junction: analysis by selective methyl phosphonate substitution. J. Mol. Biol. *343*, 851–864.
25. Bower, M., Summers, M.F., Powell, C., Shinozuka, K., Regan, J.B., Zon, G., and Wilson, W.D. (1987). Oligodeoxyribonucleoside methylphosphonates. NMR and UV spectroscopic studies of *Rp-Rp* and *Sp-Sp* methylphosphonate (Me) modified duplexes of $(d[GGAATTCC])_2$. Nucleic Acids Res. *15*, 4915–4930.
26. Loschner, T., and Engels, J.W. (1990). Diastereomeric dinucleoside-methylphosphonates: determination of configuration with the 2-D NMR ROESY technique. Nucleic Acids Res. *18*, 5083–5088.
27. Lebedev, A.V., Frauendorf, A., Vyazovkina, E.V., and Engels, J.W. (1993). Determination and prediction of the absolute configuration of dinucleoside alkylphosphonates using conformational analysis and multivariate statitics. Tetrahedron *49*, 1043–1052.
28. Chacko, K.K., Lindner, K., Saenger, W., and Miller, P.S. (1983). Molecular structure of deoxyadenylyl-3′-methylphosphonate-5′-thymidine dihydrate, (d-ApT x $2H_2O$), a dinucleoside monophosphate with neutral phosphodiester backbone. An X-ray crystal study. Nucleic Acids Res. *11*, 2801–2814.
29. Han, F., Watt, W., Duchamp, D.J., Callahan, L., Kezdy, F.J., and Agarwal, K. (1990). Molecular structure of deoxycytidyl-3′-methylphosphonate (*Rp*) 5′-deoxyguanidine, $d[Cp(CH_3)G]$. A neutral dinucleotide with Watson-Crick base pairing and a right handed helical twist. Nucleic Acids Res. *18*, 2759–2767.
30. Szabo, T., Noreus, D., Norrestam, R., and Stawinski, J. (1993). Molecular and crystal structure of S_p-thymidin-3′-yl 4-thiothymidin-5′-yl methylphosphonate. Nucleic Acids Res. *21*, 3921–3926.
31. Ha, T., Ting, A.Y., Liang, J., Caldwell, W.B., Deniz, A.A., Chemla,

D.S., Schultz, P.G., and Weiss, S. (1999). Single-molecule fluorescence spectroscopy of enzyme conformational dynamics and cleavage mechanism. Proc. Natl. Acad. Sci. USA *96*, 893–898.

32. Reynolds, M.A., Hogrefe, R.I., Jaeger, J.A., Schwartz, D.A., Riley, T.A., Marvin, W.B., Daily, W.J., Vaghefi, M.M., Beck, T.A., Knowles, S.K., et al. (1996). Synthesis and thermodynamics of oligonucleotides containing chirally pure R(P) methylphosphonate linkages. Nucleic Acids Res. *24*, 4584–4591.
33. Pöhler, J.R.G., Duckett, D.R., and Lilley, D.M.J. (1994). Structure of four-way DNA junctions containing a nick in one strand. J. Mol. Biol. *238*, 62–74.
34. Murchie, A.I.H., Thomson, J.B., Walter, F., and Lilley, D.M.J. (1998). Folding of the hairpin ribozyme in its natural conformation achieves close physical proximity of the loops. Mol. Cell *1*, 873–881.
35. Walter, N.G., Burke, J.M., and Millar, D.P. (1999). Stability of hairpin ribozyme tertiary structure is governed by the interdomain junction. Nat. Struct. Biol. *6*, 544–549.
36. Zhao, Z.-Y., Wilson, T.J., Maxwell, K., and Lilley, D.M.J. (2000). The folding of the hairpin ribozyme: Dependence on the loops and the junction. RNA *6*, 1833–1846.
37. Tan, E., Wilson, T.J., Nahas, M.K., Clegg, R.M., Lilley, D.M.J., and Ha, T. (2003). A four-way junction accelerates hairpin ribozyme folding via a discrete intermediate. Proc. Natl. Acad. Sci. USA *100*, 9308–9313.